Journal of Power Sources 257 (2014) 21–26

Contents lists available at ScienceDirect

Journal of Power Sources

journal homepage: www.elsevier.com/locate/jpowsour

Solid oxide fuel cell application in district cooling

Ayman Al-Qattan [a,*], Abdelrahman ElSherbini [b], Kholoud Al-Ajmi [a]

[a] Kuwait Institute for Scientific Research, Energy and Building Research Center, Innovative Renewable Program, P.O. Box 24885, Safat 13109, Kuwait
[b] United Technologies Research Center, 411 Silver Lane, East Hartford, CT 06108, USA

HIGHLIGHTS

- A cogeneration system based on solid oxide fuel cells is proposed for cooling and power.
- Combining district cooling with SOFC improves the cooling-to-fuel efficiency significantly.
- Thermal storage reduces capital cost by reducing the SOFC system size.
- The proposed system improves efficiency by up to 346%, and reduces CO_2 by 54%.
- The total cost to produce one unit of cooling is 53% less than current practice.

ARTICLE INFO

Article history:
Received 15 September 2013
Received in revised form
28 December 2013
Accepted 3 January 2014
Available online 31 January 2014

Keywords:
Cogeneration
Solid oxide fuel cell
District cooling
Thermal storage
Air-conditioning
Coefficient of performance

ABSTRACT

This paper presents analysis of the performance of a combined cooling and power (CCP) system for district cooling. The cogeneration system is designed to provide cooling for a low-rise residential district of 27,300 RT (96 MWc). A solid oxide fuel cell (SOFC) generates electric power to operate chillers, and the exhaust fuel and heat from the SOFC run gas turbines and absorption chillers. Thermal energy storage is utilized to reduce system capacity. Part-load operation strategies target maximizing energy efficiency. The operation of the system is compared through an hourly simulation to that of packaged air-conditioning units typically used to cool homes. The CCP system with the district cooling arrangement improves the cooling-to-fuel efficiency by 346%. The peak power requirement is reduced by 57% (24 MW) and the total fuel energy is reduced by 54% (750 TJ y^{-1}). The system cuts annual carbon dioxide emissions to less than half and reduces other harmful emissions. A cost analysis of the system components and operation resulted in a 53% reduction in the cost per ton-hour of cooling over traditional systems.

1. Introduction

In hot climates, a considerable share of end-use energy is consumed to provide comfort cooling. For example, air-conditioning (A/C) in Kuwait accounts for nearly 70% of the electricity demand during peak hours and 45% of the annual consumption. For the residential sector, the shares of A/C reach 85% of peak power and 55% of annual consumption. In addition to the high costs of power generation and distribution, high rates of greenhouse gases and harmful emissions are released. This article analyzes a high-efficiency low-emission system for combined cooling and power (CCP) for a district cooling application.

Several studies on cogeneration had focused on the performance of systems with microturbines. Ho et al. [1] experimentally evaluated the performance of a cogeneration system designed to provide electrical power and space cooling to a laboratory. The system's technical configuration included a Capstone microturbine, a 10-RT (35 kW) Yazaki absorption chiller, two heat exchangers, a propane fuel supply system, and a cooling tower. The results from the performance tests showed that the microturbine electrical efficiency was 21% at near full load of 24 kW whilst the chiller operated with coefficient of performance (COP) ranging from 0.5 to 0.58, depending on the electrical output. The overall system efficiency ranged from 40% to 49%.

Another interesting investigation, Kong et al. [2], experimentally studied a combined cooling, heating and power (CCHP) microsystem consisting of a small-scale generator set driven by a gas engine and a new small-scale silica–water adsorption chiller. The system can supply 12 kW electrical power, 28 kW heating power, or 9 kW refrigeration power simultaneously with overall electrical and thermal efficiency over 70%.

* Corresponding author. Tel.: +965 24989258; fax: +965 24989139.
E-mail addresses: aqattan@kisr.edu.kw, aqattan@gmail.com (A. Al-Qattan).

0378-7753/$ – see front matter © 2014 Elsevier B.V. All rights reserved.
http://dx.doi.org/10.1016/j.jpowsour.2014.01.099

Moya et al. [3] presented a detailed experimental analysis of an advanced trigeneration system designed to operate with a natural gas microturbine, air-cooled absorption chiller that uses ammonia or water, and a heat recovery boiler. In their work, the micro gas turbine provided up to 28 kW of electrical power and 60 kW of heat to derive the absorption chiller with 17 kW nominal cooling capacity. Detailed analysis results revealed that the COP and capacity of the chiller were influenced by the indirect effect of the ambient temperature on the micro gas turbine, and its direct effect on the condenser and the absorber of the chiller. At high ambient temperatures over 40 °C, the chiller capacity is reduced by 0.5 kW $°C^{-1}$.

Power generation using fuel cells is a promising alternative to traditional turbines. The main advantages of fuel cells include high efficiency, low emissions, quietness and modularity. Such features are well suited for distributed generation applications, where the efficiency can be further enhanced by utilizing the released heat. In hot regions, that extra energy is needed for cooling.

Silveira et al. [4] and Leal and Silveira [5] analyzed the use of fuel-cell cogeneration systems for cooling utilizing molten carbonate fuel cells (MCFC). The results manifested the potential of such technology for cooling. Burer et al. [6] investigated the optimization of a multicomponent system for district heating, cooling, and power generation. The complex system integrated a combined fuel-cell gas-turbine cycle with compression and absorption chillers and a heat pump. The system was optimized for cost and carbon dioxide (CO_2) emissions.

In an assessment study, Dorer et al. [7] evaluated the performance of micro-cogeneration systems for residential buildings. The study assessed two types of natural gas driven fuel cell systems (SOFC and polymer electrolyte membrane fuel cell (PEMFC)). The results showed that the fuel-cells-based systems achieved reductions of 6–48% in the primary energy demand of buildings.

Zink et al. [8] analyzed an SOFC system with absorption cooling and heating for buildings. They reported a total system efficiency of up to 95%. Darwish [9] presented a case study for using phosphoric acid fuel cell (PAFC) systems to produce cooling. The analysis suggested that FC-based A/C systems would result in significant savings if target system costs are reached.

In an earlier work [10], the authors introduced an integrated cogeneration system based on SOFC, which was designed to provide cooling and power. In another study, Clausse et al. [11] explored the theoretical performance of a natural gas fuel cell system with adsorption-based air conditioning. The researchers analyzed the performance for three different adsorption pairs: activated carbon and methanol, silica gel and water, and zeolite and water. They found that the zeolite and water pair showed the best cooling performance.

Calise et al. [12] presented a dynamic model combining solar heating and cooling technologies with PEMFCs. The system included evacuated solar collectors, single-stage lithium bromide (LiBr) absorption chiller and PEMFC. Their model showed that the maximum operating temperature of the PEMFC (80 °C) was too low to derive the absorption chiller at high COP. They suggested using high temperature fuel cells (SOFC), combined with parabolic trough collectors and double stage absorption chillers.

In a recent study, Guizzi et al. [13] analyzed the annual energy consumption, operating cost and CO_2 emissions of a distributed generation plant based on a PEMFC with a vapor compression chiller. The results showed that the annual energy cost was reduced by 47% when the thermal energy from the system was usefully recovered. An absorption chiller was not used because most of the heat was recovered at low temperatures. In that study, the authors did not consider high temperature fuel cells, which could solve this problem and provide even more energy savings. Takezawa et al. [14] studied a high temperature SOFC-gas-turbine system and analyzed the use of absorption chillers to recover the exhaust heat. They found that a double effect absorption chiller would produce less than 10% additional capacity than a single effect chiller.

The goal of the present work is to evaluate the performance of a fuel cell air conditioning (FCAC) system for a large district cooling application at various loading scenarios. The system combines high temperature fuel cells with gas turbines and various cooling technologies to maximize energy efficiency. The paper also assesses the cost effectiveness of the system for such an application.

2. System description

The integrated FCAC system targets improvements in energy efficiency at the generation, distribution and utilization stages. It consists of an SOFC, a gas turbine, absorption and compression chillers and a thermal storage tank, as shown in Fig. 1. The SOFC converts fuel energy into electricity. The exhaust heat is used to generate more electricity and to drive absorption chillers. The generated electricity runs vapor compression chillers. The integrated system primarily supplies chilled water to a district cooling network, which delivers cooling to individual homes and buildings. A thermal energy storage tank is utilized to reduce the required cooling capacity of the system. This FCAC system is designed to provide sufficient cooling for the district it serves during peak summer. For periods of lower cooling demand, the system will feed extra electricity to the grid.

The FCAC system can be divided into a power generation subsystem that includes the SOFC and the gas turbine, and a cooling subsystem that includes the absorption and compression chillers, their auxiliaries and the thermal storage tank. The key parameters for the power generation subsystem and the cooling subsystem are summarized in Tables 1 and 2, respectively. For this analysis, the SOFC was selected to have a tubular design, which allows for pressurized operation (3 bar). The cell operating temperature is 1000 °C. For the cooling subsystem, the temperature differential between the leaving and returning chilled water was slightly higher than typical. This is a common practice in district cooling applications to reduce the power needed to pump chilled water. Also, the cooling tower water temperature was high, due to the hot climate of the region.

3. Analysis

3.1. System model

A model for the power generation subsystem was developed. The model calculates the fuel cell voltage and current density, power produced, the composition and temperature of the mixture at

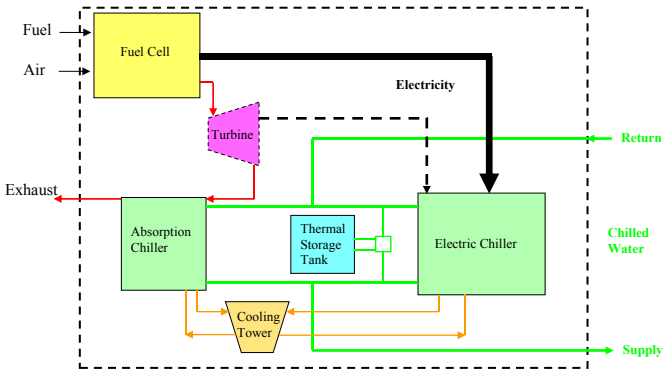

Fig. 1. The proposed integrated fuel cell air conditioning (FCAC) system.

Table 1
Key parameters for the power generation subsystem.

Parameter	Value
Fuel cell type	Tubular SOFC
Cell diameter (mm)	22
Cell length (mm)	1500
Anode thickness (μm)	100
Cathode thickness (mm)	2.2
Electrolyte thickness (μm)	40
Interconnection thickness (μm)	85
Number of cells	48,120
Cell operating temperature (°C)	1000
Cell operating pressure (bar)	3
Steam-to-fuel ratio	1.255
Air-to-fuel ratio	26.6
Fuel utilization (%)	80
Fuel recirculation ratio	0.235
Fuel inlet mixture composition	100% CH_4
Air inlet mixture composition	21% O_2 and 79% N_2
Compressor efficiency (%)	85
Turbine efficiency (%)	90

the turbine outlet and the efficiency of the subsystem. The power subsystem, shown in Fig. 2, consists of a tubular SOFC with fully internal reforming, prereformer, two mixers, three heat exchangers, two compressors, a pump, a complete combustor and a turbine.

In the steady state model, mass and energy balances are applied to each component to evaluate the temperature and the composition at the exit of that component. The exit flow for each component is considered as the inlet flow for the next one.

The mass flow rate of fuel is considered as an operating variable. The cell operating temperature and pressure are defined as external parameters. The fuel utilization factor, steam to fuel ratio, air to fuel ratio and fuel recirculation ratio are kept constant. The internal distribution of temperature, gas composition and pressure in each component are neglected. Ideal gases are assumed to have no leakage and no pressure drop. Reforming and shifting reactions are assumed to be at equilibrium. The temperatures of the anode and cathode exits are considered equal to the solid cell temperature. More details about the fuel-cell-turbine model can be found in Al-Qattan et al. [15].

The cooling generation subsystem consists of absorption chillers, electric chillers, pumps, cooling towers and thermal storage tanks. The exhaust of the turbine is fed to double-effect water/LiBr absorption chillers. The integration between the turbine exhaust and the absorption chillers was examined. The power generation model showed the turbine exhaust to consist mainly of air with some CO_2 (5% by mass) and steam (7% by mass). The exhaust can be directly fed into the absorption chiller, providing heat to the high pressure desorber. Alternatively, the exhaust can pass through a heat exchanger to heat steam which feeds steam-fired absorption chillers.

Table 2
Key parameters for the cooling subsystem.

Component	Parameter	Value
Electric chiller	Chiller type	Water cooled
Electric chiller	Rated efficiency (kW RT^{-1})	0.61
Electric chiller including auxiliaries (water pumps and cooling tower fans)	Efficiency (kW RT^{-1})	0.87
Electric chiller	Leaving chilled water temperature (°C)	6.1
Electric chiller	Entering chilled water temperature (°C)	12.8
Absorption chiller	Chiller type	Double effect, water cooled
Absorption chiller	COP (kWc kWe^{-1})	1.3
Cooling tower	Entering water temperature (°C)	40
Cooling tower	Leaving water temperature (°C)	35
PAC unit (for comparison)	Rated efficiency, excluding fans (kW RT^{-1})	1.255

The electrical efficiency of the power generation subsystem is expressed as

$$\eta_{FCT} = W_{FCT}/Q_F \quad (1)$$

where W_{FCT} is the net power output of the power generation subsystem and Q_F is the rate of energy input by fuel. The net power is the output of the fuel cell and turbine minus the input work of the air and fuel compressors and the water pump. The rate of energy input, Q_F, is equal to the mass flow rate of fuel times its lower heating value (LHV). Natural gas is a convenient fuel for the SOFC.

The overall efficiency of the FCAC system, COP_{sys}, can be calculated from

$$COP_{sys} = (Q_{e,vcc} + Q_{e,abs})/Q_F \quad (2)$$

where $Q_{e,abs}$ is the amount of cooling at the evaporator of the absorption chiller and $Q_{e,vcc}$ is the amount of cooling produced by the compression chiller.

3.2. Application and system operation

The application for district cooling was selected for a new city in Kuwait. The district consists of a block with 805 residential villas, 4 schools, 2 community shopping centers and 4 houses of worship. A typical villa has an air-conditioned area of 800 m^2. The cooling load requirements for the district were estimated to be 27,300 RT (96 MW).

The system operation strategy seeks to meet the cooling load at high efficiency. At design conditions, the electrical output of the fuel cell and turbine is fully utilized for running the vapor-compression chiller. The captured heat from the exhaust operates the absorption chiller at its rated capacity. The combined capacity of the electric and absorption chillers is augmented by the cooling from the thermal storage tank to meet the design cooling load. When the cooling demand is less than the design load, the operation of the FCAC aims at maintaining high efficiency and power output.

Historical and present weather and load data are used to predict the cooling demand for the day. On hot summer days, thermal storage and retrieval may be needed to augment the chillers' capacity for a few hours. At any given time, the present capacity of the storage tank is assessed and the quantity of cooling to be stored (if any) is added to the current cooling demand to yield the total cooling requirement.

When the total cooling requirement is higher than the rated capacity of the absorption chiller, the fuel cell and absorption chiller are operated at rated capacities, and the vapor-compression chiller delivers the remainder of the cooling duty. When the electric chiller operates below the rated capacity, the extra power generated by the system is fed to the grid. The power delivered to the grid, W_g, is

$$W_g = W_{FCT} - W_{vcc} \quad (3)$$

where W_{FCT} is the net power output of the power subsystem and W_{vcc} is the power consumed by the vapor-compression chiller and auxiliaries.

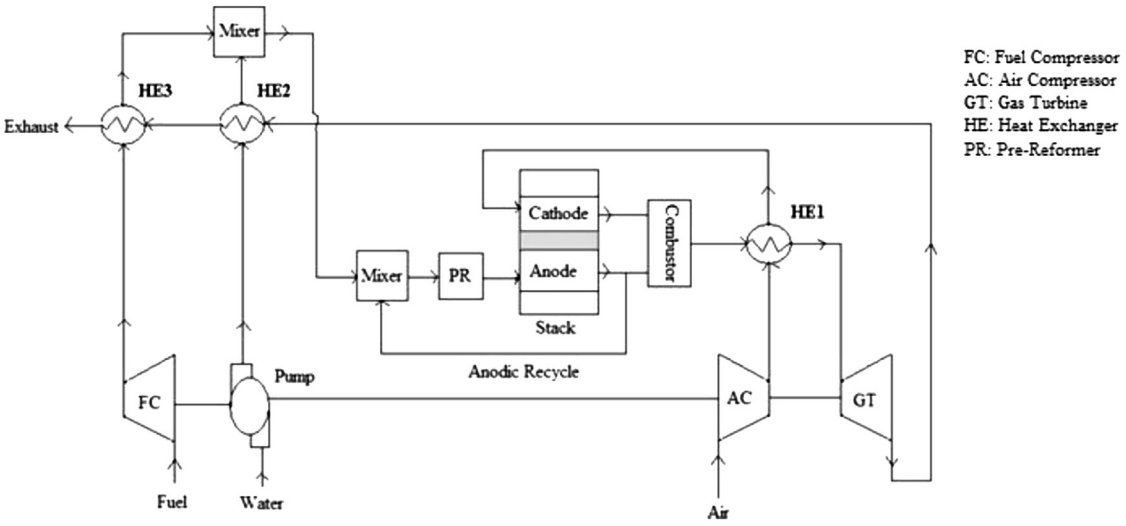

Fig. 2. A schematic diagram of the power generation subsystem.

For a total cooling requirement below the rated capacity of the absorption chiller, that chiller is run at part-load to meet the requirement. In this case, the vapor-compression chiller is kept off and the fuel cell is partially operated to generate sufficient heat for absorption. Since $W_{vcc} = 0$, all the generated power goes to the grid. If thermal storage is needed, chilled water is charged to the storage tank. Conversely, if the quantity of cooling from chillers is insufficient, chilled water from the tank is utilized for meeting the required duty. Due to the hot climate, the long cooling season extends from March to November. The system will be shut down from December to February, due to the low energy demand and negligible space heating requirements. This policy can extend the calendar life of the system.

4. Results and discussion

The sizing of the FCAC system and its performance are analyzed based on the aforementioned models. The analysis showed the electrical efficiency of the hybrid fuel cell/turbine sub-system to be 60.8%. An efficient vapor compression chiller is selected for the FCAC system. Electric chiller efficiencies are commonly expressed in terms of power rating, which is the input power in kW divided by cooling capacity in RT. In order to reduce the pumping power for district cooling, a high temperature differential is maintained between chilled water supply and return. When power requirements for chilled water pumps, condenser water pumps and cooling tower fans are added to the chiller's power requirement, the power rating is estimated to be 0.87 kW RT^{-1}. Thus, the coefficient of performance for the compression chiller, COP_{vcc}, is taken as 4.04. This value excludes the power requirements of the air-distribution system at individual homes, which will be supplied by the electrical grid. The COP for the selected water–LiBr absorption chiller is 1.3. Both the electric and absorption chillers are commercially available products.

The thermal storage tank is sized based on the cooling load for the district. The analysis of the hourly cooling profile during the peak summer shows that the daily average load does not exceed 72% of the peak. Thus, the chillers were sized with a margin of safety to provide 85% of the peak load. The remaining capacity will be provided, when needed, by the thermal storage tanks.

An hour-by-hour simulation of the operation of the FCAC system was conducted to assess its performance. Using a numerical solver, the operation strategy was applied to the hourly cooling load of the district to estimate the total energy consumption of the system per year.

The original design of the residential district uses packaged air-conditioning (PAC) units to provide cooling for all buildings. A PAC unit is selected to compare the performance of existing and proposed systems. The coefficient of performance for the PAC unit, COP_{PAC}, is

$$COP_{PAC} = Q_{e,PAC}/W_{PAC} \quad (4)$$

where $Q_{e,PAC}$ is the cooling in kW and W_{PAC} is the power in kW. For comparison with the FCAC system, this COP excludes air distribution. Thus, the power for the fan and the heat it adds are not included. The rated COP of the selected PAC unit is 2.80. However, the efficiency of PAC systems is sensitive to ambient temperature, since they are air-cooled. Based on manufacturer's performance data, a relation between COP_{PAC} and ambient temperature is used to calculate the energy consumption of PAC units at any time. The coefficient of performance for Kuwait design conditions, excluding air distribution, drops to 2.29. In order to compare with the FCAC system, the fuel-based coefficient of performance (COP_F) is calculated as

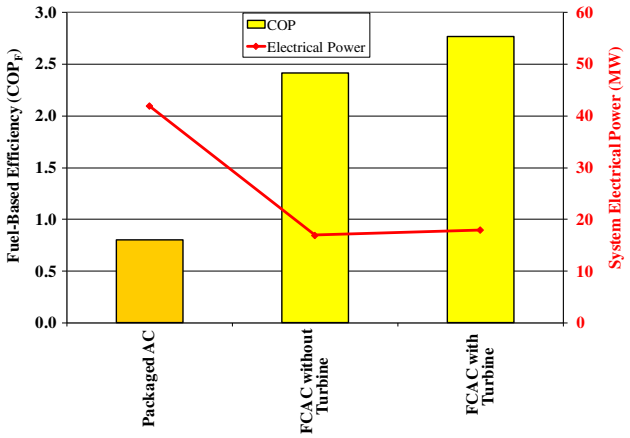

COP =Coefficient of Performance; AC = air-conditioning; FCAC = fuel cell air conditioning;

Fig. 3. Efficiency and power of the FCAC system compared to the existing systems.

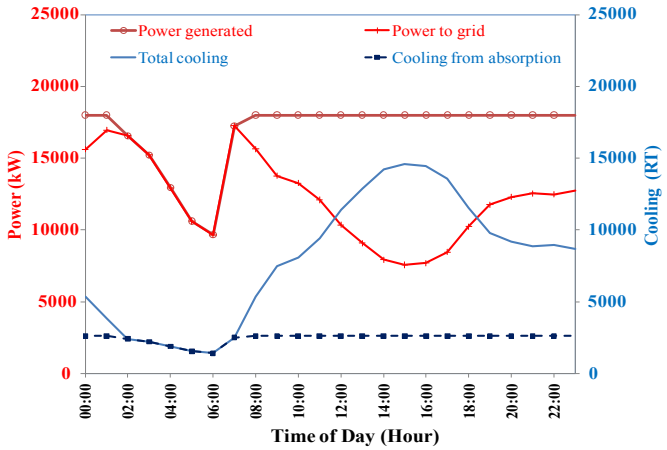

Fig. 4. Power and cooling for a selected day in April.

$$COP_F = \eta_{PP} \cdot COP_{PAC} \quad (5)$$

where η_{PP} is the efficiency of the power plant. The majority of power in Kuwait is generated by steam power plants, with efficiency of 39%. When electrical distribution losses are accounted for, the value of η_{PP} is 35%. Therefore, the fuel-based COP for PAC systems is 0.80.

Fig. 3 compares the efficiency and power requirements of the existing systems to those of the FCAC system. The proposed system improves the fuel-based efficiency over PAC units from 0.8 to 2.77, a 346% enhancement. The power requirement is reduced from 41.9 to 18 MW, a 57% reduction. Fig. 3 also shows the power and efficiency for a different configuration where the turbine is removed from the power generation subsystem. This configuration has lower COP and lower power because of the decreased electrical efficiency. In this case, the rated capacity of the electric chiller is reduced and that of the absorption chiller is increased.

The part-load operation of the system is manifested by showing the low and high cooling demands on two days as example. Fig. 4 shows the power and cooling for a selected day in April. The total cooling demand ranges between 1400 and 14,600 RT (4.9 and 51.34 MW). The cooling demand between 2:00 h and 7:00 h is less than the capacity of the absorption chiller. The fuel cell is run at part-load, so that the exhaust heat meets the requirement of the

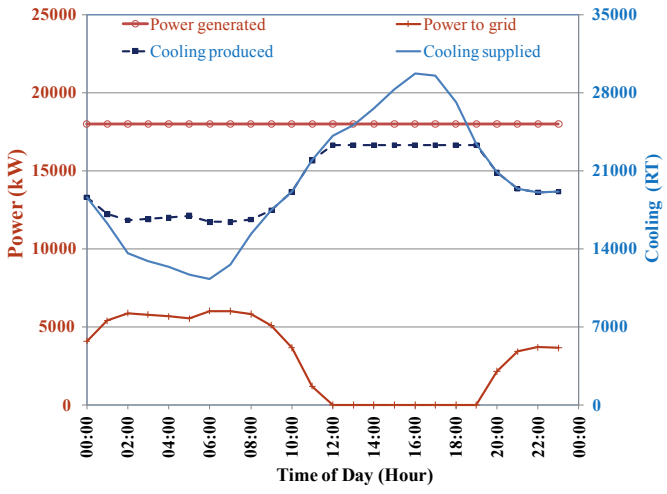

Fig. 5. Power and cooling for a selected day in August.

Table 3
Summary of capacities and consumption for the FCAC and PAC systems.

	Units	System		Improvement %
		PAC	FCAC	
District size	RT	27,300	27,300	
Chillers capacity – total	RT	–	23,300	
Compression chillers	RT	–	20,680	
Absorption chillers	RT	–	2620	
TES tank size	RT h	–	20,868	
Rated power	MW	41.9	18	57
COP_F		0.8	2.77	346
Fuel consumption	TJ y^{-1}	1389	641	54
Electricity to grid	GWh y^{-1}	–	59.1	

FCAC = fuel cell air conditioning; PAC = packaged air-conditioning; COP_F = coefficient of performance based on fuel.

absorption chiller. The power generated by the fuel cell during that period is fed to the grid. For the rest of the day, the cooling demand is higher and the electric chiller generates the remainder of the cooling. As the total cooling demand increases during afternoon hours, W_{vcc} increases and W_g decreases accordingly.

Fig. 5 shows the power and cooling for a selected day in August. The cooling demand reaches a peak of 26,878 RT (94.53 MW), which is beyond the chillers' total capacity of 23,300 RT (81.94 MW). During the early hours of the day, additional cooling is produced and stored in the tank. For the duration of 11:00 to 18:00 h, chillers are run at full capacity, and the storage tank meets the remainder of the cooling demand. In this case, the system consumes all the electricity it generates ($W_g = 0$). However, the FCAC system still feeds electricity to the grid that day during hours of lower cooling demand.

The annual operation of the FCAC system was compared to that of PAC systems. Table 3 summarizes the sizing results and the power and energy consumption for the FCAC system and PAC systems. The FCAC system delivered 59.1 GWh of electricity to the grid while meeting the annual cooling demand of the district. The total fuel energy of the FCAC during the 9-month period of operation was 641 TJ. In contrast, the fuel energy required by traditional systems to meet the cooling demand and deliver a similar amount of electricity was 1389 TJ. Thus, over the period of its operation, the FCAC saved 54% of the fuel energy. This fuel saving is translated to reductions in CO_2 emissions, in addition to the considerable reductions in sulfur oxides (SO_x) and nitrogen oxides (NO_x) due to the use of fuel cells.

A cost-benefit analysis was conducted to assess the economic effectiveness of the proposed system. Cost functions were formulated for each component, based on the analysis of Arsalis [16], and expressed as annual capital and annual operating costs. The cost of the SOFC was based on market studies for the case of large volumes of production [16]. Details of component costs are available in Al-

Table 4
Cost comparison between the proposed and traditional systems.

	Unit	FCAC		PAC
Cooling	RT h y^{-1}	72,190,215		72,190,215
Capital cost	\$ y^{-1}	DC system	2,787,872	1,568,966
		Power gen	1,087,376	
Operating cost	\$ y^{-1}	DC system	2,406,218	8,909,179
		Power gen	5,526,241	
Total cost	\$ y^{-1}	11,807,707		10,478,145
Savings due to generated electricity	\$ y^{-1}	6,924,310		0
Net cost	\$ y^{-1}	4,883,397		10,478,145
Cost per ton-hour	\$ RT^{-1} h^{-1}	0.0676		0.1452

FCAC = fuel cell air conditioning; DC = district cooling.

Qattan et al. [15]. For the power generation subsystem, the highest capital cost went for the SOFC, followed by the turbine, while the highest operating cost was that of fuel. On the other hand, the highest capital cost of the cooling subsystem was for piping, due to the horizontal stretch of the district with low density of cooling demand. The highest operating cost of cooling was for water used in cooling towers, due to the high cost of water production in Kuwait.

The cost of the integrated FCAC system was compared to that of the traditional PAC system. The total annual cost for each system was divided by the annual amount of cooling produced to obtain the cost per ton-hour ($ RT^{-1} h^{-1}). The total cost includes capital and operating costs on an annual basis. For the PAC system, the capital cost refers to the cost of the A/C units and the operating cost was mainly for electricity. The current cost of electricity for the government in Kuwait is \$0.117 kWh^{-1}. For the FCAC system, the cost included the district cooling and power generation subsystems. The natural gas price was taken as \$5/MSCF (\$0.177 m^{-3}), and the government cost of water in Kuwait as \$16/1000 gallons. The price of electricity fed to the grid was subtracted from the cost to obtain a net cost. Table 4 compares the costs of FCAC and PAC systems. The cost of \$0.0676 RT^{-1} h^{-1} (\$0.0192 kWh^{-1}) for the FCAC was 53% lower than that for the PAC system.

5. Conclusions

The performance of a fuel-cell-based combined cooling and power system was studied for a district cooling application. The system consisted of a hybrid SOFC with gas turbine, absorption and electric chillers with their auxiliaries and a thermal storage tank. The FCAC system was designed to meet the cooling demands of the district, and to feed extra electricity to the grid during periods of lower demand. The performance of the system was simulated on an hourly basis and compared to that of traditional PAC units. The FCAC system improved the fuel-based efficiency of cooling production by 346% and reduced peak power requirements by 24 MW, or 57%. Fuel consumption and CO_2 emissions were reduced by 54%. A detailed cost analysis of the system components and their operation showed the cost of delivering one RT h of cooling to be 53% lower than that by traditional PAC systems.

Abbreviations

CCP	combined cooling and power
SOFC	solid oxide fuel cell
A/C	air-conditioning
COP	coefficient of performance
CCHP	combined cooling, heating and power
MCFC	molten carbonate fuel cells
PAFC	phosphoric acid fuel cell
PEMFC	polymer electrolyte membrane fuel cell
FCAC	fuel cell air conditioning
LHV	lower heating value
PAC	packaged air-conditioning

References

[1] J.C. Ho, K.J. Chua, S.K. Chou, Renew. Energy 29 (2004) 1121–1133.
[2] X.Q. Kong, R.Z. Wang, J.Y. Wu, X.H. Huang, Y. Huangfu, D.W. Wu, Y.X. Xu, Int. J. Refrig. 28 (2005) 977–987.
[3] M. Moya, J.C. Bruno, P. Eguia, E. Torres, I. Zamora, A. Coronas, Appl. Energy 88 (2011) 4424–4440.
[4] J.L. Silveira, E.M. Leal, L.F. Ragonha, Energy 26 (2001) 891–904.
[5] E.M. Leal, J.L. Silveira, J. Power Sources 106 (2002) 102–108.
[6] M. Burer, K. Tanaka, D. Favrat, K. Yamada, Energy 28 (2003) 497–518.
[7] V. Dorer, R. Weber, A. Weber, Energy Build. 37 (2005) 1132–1146.
[8] F. Zink, Y. Lu, L. Schaefer, Energy Convers. Manag. 48 (2007) 809–818.
[9] M.A. Darwish, Appl. Therm. Eng. 27 (2007) 2869–2876.
[10] A. ElSherbini, A. Al-Qattan, in: Sixth International Fuel Cell Science, Engineering and Technology Conference, Denver, CO, USA, June 16–18, 2008.
[11] M. Clausse, F. Meunier, J. Coulie, E. Herail, Int. J. Refrig. 32 (2009) 712–719.
[12] F. Calise, G. Ferruzzi, L. Vanoli, Energy 41 (2012) 18–30.
[13] G.L. Guizzi, M. Manno, Energy 41 (2012) 56–64.
[14] S. Takezawa, K. Wakahara, T. Araki, K. Onda, S. Nagata, Electr. Eng. Jpn. 167 (2009) 49–55.
[15] A. Al-Qattan, A. ElSherbini, K. AlAjmi, Design of Fuel Cell-based Cogeneration Systems for Cooling and Power in Buildings, EU035K, KISR Report, Kuwait, 2010.
[16] A. Arsalis, J. Power Sources 181 (2008) 313–326.